J|A|C|S ARTICLES

Published on Web 11/24/2009

Nanoscale 3D Tracking with Conjugated Polymer Nanoparticles

Jiangbo Yu, Changfeng Wu, Sushant P. Sahu, Lawrence P. Fernando, Craig Szymanski, and Jason McNeill*

Department of Chemistry and Center for Optical Materials Science and Engineering Technologies, Clemson University, Clemson, South Carolina 29634

Received August 26, 2009; E-mail: mcneill@clemson.edu

Abstract: Small (~15 nm diameter), highly fluorescent conjugated polymer nanoparticles were evaluated for nanoscale 2D and 3D tracking applications. Nanoparticles composed of conjugated polymers possess high absorption cross sections, high radiative rates, and low or moderate aggregation quenching, resulting in extraordinarily high fluorescent brightness. The bright fluorescence (~200 000 photons detected per particle per 20 ms exposure) yields a theoretical particle tracking uncertainty of less than 1 nm. A lateral tracking uncertainty of 1−2 nm was determined from analysis of trajectories of fixed and freely diffusing particles. Axial (*Z*) position information for 3D particle tracking was obtained by defocused imaging. Nanoscale tracking of single particles in fixed cells was demonstrated, and a range of complex behaviors, possibly due to binding/unbinding dynamics, were observed.

Introduction

Nanoscale 2D and 3D single particle tracking methods have proven to be extraordinarily useful for investigating a wide variety of cellular processes such as molecule transport, membrane dynamics, and the motion of motor proteins.[1−6] There is considerable interest in improving the spatial and temporal resolution of tracking methods. While the positions of isolated, tethered single dye molecules can be determined with ~1.5 nm accuracy,[1] the low brightness and fluorescence emission rates of a single dye molecule place severe constraints on time resolution and intracellular studies. Strategies for improving the spatiotemporal resolution of particle tracking experiments include the use of multiple labeling with dyes or fluorescent proteins,[7] fluorescent nanoparticles such as colloidal semiconductor quantum dots and dye-loaded nanospheres,[2−4] and highly scattering metal nanoparticles. However, dye-loaded nanoparticles and metal nanoparticles are typically larger than 20−30 nm, which can affect biological function, and their hydrodynamic drag places an effective limit on temporal resolution. Individual colloidal semiconductor quantum dots yield limited resolution at acquisition rates above 50 Hz due to saturation effects.[3,6] Based on these considerations, it appears that the development of more highly luminescent nanoparticles with diameters in the range of 5−20 nm is needed to improve the spatial and temporal resolution of particle tracking methods.

We recently developed brightly fluorescent nanoparticles, here referred to as CPNs, that consist of one or more π-conjugated polymer molecules.[9−12] In contrast to dye-doped polymer or silica beads, which are typically limited to a few percent dye loading due to aggregation and self-quenching effects,[13] CPNs are entirely composed of fluorescent polymer, resulting in markedly higher absorption cross sections. In addition, many conjugated polymers exhibit minimal self-quenching, with reported fluorescence quantum yields of 70% for pure solid films,[14] while CPN fluorescence quantum yields as high as 40% have been determined.[12] CPNs can be prepared with diameters ranging from 4 nm (a single polymer molecule) to >50 nm, with particle brightness scaling approximately linearly with nanoparticle volume over this size range, which permits the optimization of the particle size−brightness trade-off for a

(1) Yildiz, A.; Forkey, J. N.; McKinney, S. A.; Ha, T.; Goldman, Y. E.; Selvin, P. R. *Science* **2003**, *300*, 2061–2065.
(2) Dahan, M.; Levi, S.; Luccardini, C.; Rostaing, P.; Riveau, B.; Triller, A. *Science* **2003**, *302*, 442–445.
(3) Murcia, M. J.; Minner, D. E.; Mustata, G.-M.; Ritchie, K.; Naumann, C. A. *J. Am. Chem. Soc.* **2008**, *130*, 15054–15062.
(4) Toprak, E.; Balci, H.; Blehm, B. H.; Selvin, P. R. *Nano Lett.* **2007**, *7*, 2043–2045.
(5) (a) Huang, B.; Wang, W. Q.; Bates, M.; Zhuang, X. W. *Science* **2008**, *319*, 810–813. (b) Levi, V.; Ruan, Q. Q.; Gratton, E. *Biophys. J.* **2005**, *88*, 2919–2928. (c) Lessard, G. A.; Goodwin, P. M.; Werner, J. H. *Appl. Phys. Lett.* **2007**, *91*, 224106/1–224106/3. (d) Greenleaf, W. J.; Woodside, M. T.; Block, S. M. *Annu. Rev. Biophys. Biomol. Struct.* **2007**, *36*, 171–190.
(6) Holtzer, L.; Meckel, T.; Schmidt, T. *Appl. Phys. Lett.* **2007**, *90*, 053902/1–053902/3.
(7) Kural, C.; Kim, H.; Syed, S.; Goshima, G.; Gelfand, V. I.; Selvin, P. R. *Science* **2005**, *308*, 1469–1472.
(8) (a) Sheetz, M. P.; Turney, S.; Qian, H.; Elson, E. L. *Nature* **1989**, *340*, 284–288. (b) Kusumi, A.; Sako, Y.; Yamamoto, M. *Biophys. J.* **1993**, *65*, 2021–2040.
(9) (a) Szymanski, C.; Wu, C. F.; Hooper, J.; Salazar, M. A.; Perdomo, A.; Dukes, A.; McNeill, J. *J. Phys. Chem. B* **2005**, *109*, 8543–8546. (b) Wu, C.; Szymanski, C.; Cain, Z.; McNeill, J. *J. Am. Chem. Soc.* **2007**, *129*, 12904–12905.
(10) (a) Wu, C.; Peng, H.; Jiang, Y.; McNeill, J. *J. Phys. Chem. B* **2006**, *110*, 14148–14154. (b) Wu, C.; Zheng, Y.; Szymanski, C.; McNeill, J. *J. Phys. Chem. C* **2008**, *112*, 1772–1781.
(11) Wu, C.; Szymanski, C.; McNeill, J. *Langmuir* **2006**, *22*, 2956–2960.
(12) Wu, C.; Bull, B.; Szymanski, C.; Christensen, K.; McNeill, J. *ACS Nano* **2008**, *2*, 2415–2423.
(13) (a) Jungmann, N.; Schmidt, M.; Ebenhoch, J.; Weis, J.; Maskos, M. *Angew. Chem., Int. Ed.* **2003**, *42*, 1714–1717. (b) Zhao, X. J.; Bagwe, R. P.; Tan, W. H. *Adv. Mater.* **2004**, *16* (2), 173–176.
(14) Pei, Q. B.; Yang, Y. *J. Am. Chem. Soc.* **1996**, *118*, 7416–7417.

10.1021/ja907228q

particular application. In addition, the excitation wavelength is readily tailored to a specific application by choosing from a wide variety of commercially available π-conjugated polymers, and highly red-shifted emission can be achieved by energy transfer to dopant dyes or polymers.[10] For particles in the 5−50 nm range, CPNs can achieve arguably the highest fluorescence brightness to volume ratio of any nanoparticle reported to date; a fluorescence cross section of 2.2×10^{-13} cm^2 and saturated emission rates of 10^9 photons per particle per second were observed for CPNs ∼15 nm in diameter. CPN encapsulation and functionalization have been demonstrated, indicating the possibility of nanoparticle conjugation to specific biomolecules.[11] Additionally, highly photostable CPNs, ∼1000 times more photostable than conventional dyes, have been demonstrated.[12] Furthermore, CPNs do not contain toxic heavy metals, which are a concern for some applications.

In this study, we evaluate the use of single ∼15 nm diameter CPNs for 2D and 3D tracking at an acquisition rate of 50 Hz. From the signal levels of isolated nanoparticles, a theoretical tracking uncertainty of better than 1 nm is estimated. An experimental tracking uncertainty of 1−2 nm is obtained from tracking analysis performed on stationary particles. 2D and 3D tracking of particles undergoing Brownian motion in glycerol is demonstrated, and an estimated tracking uncertainty of less than 5 nm in the *xy* plane and ∼20 nm along the *z* axis is determined. Intracellular particle tracking is also demonstrated, and particle trajectories are found to be consistent with expected phenomena such as partially confined diffusion and reversible and irreversible binding to the cell components. The tracking results indicate that CPNs are promising for measuring the local diffusivity and nanoscale motion of individual biomolecules and subcellular structures in cells.

Experimental Section

Nanoparticle Preparation and Characterization. The polyfluorene derivative PFBT (MW 10,000, polydispersity 1.7) was purchased from ADS Dyes, Inc. (Quebec, Canada). Tetrahydrofuran (THF, HPLC grade, 99.9%) and glycerol (99.5%) were purchased from Sigma-Aldrich (Milwaukee, WI). All chemicals were used without further purification. For preparation of PFBT nanoparticles, 10 mg of the conjugated polymer PFBT were dissolved in 10 g of HPLC grade tetrahydrofuran (THF) by stirring overnight under an inert atmosphere. The solution was then filtered through a 0.7 μm glass fiber filter to remove any insoluble material. Then 200 μL of the solution were injected by pipet into 8 mL of water under mild sonication. The THF was removed by partial vacuum evaporation, and aggregates were removed by filtration through a 220 nm PTFE membrane filter. Typically, less than 10% of the polymer was removed by filtration, as determined by UV−vis, indicating that most of the polymer formed nanoparticles. A suspension of PFBT nanoparticles in glycerol was prepared by mixing the aqueous nanoparticle suspension with glycerol, followed by partial vacuum evaporation at 70 °C to remove the water. For the determination of particle size by AFM, one drop of the nanoparticle dispersion was placed on a freshly cleaved mica substrate. After evaporation of the water, the surface topography was imaged with an Ambios Q250 AFM in AC mode, yielding a size range of 14.9 ± 4.9 nm (histogram provided in the Supporting Information). A zeta potential of −46.7 mV was determined by electrophoretic light scattering (Zetasizer Nano ZS, Malvern Instruments). UV−vis absorption spectra of PFBT in THF and aqueous suspensions of PFBT nanoparticles were recorded with a Shimadzu UV-2101PC scanning spectrophotometer using 1 cm quartz cuvettes, and fluorescence spectra were recorded using a commercial fluorometer (Quantamaster, PTI, Inc.). Nanoparticle optical absorption cross sections were estimated from the absorbance of solutions at a known weight fraction, and estimates of the nanoparticle mass were based on the nanoparticle diameter and polymer density. Nanoparticle fluorescence quantum yields were determined from UV−vis and fluorescence spectra using Coumarin 6 as a standard.

Cell Culture. For the cell imaging experiments, mouse macrophage-like J774.A1 cells (ATCC, Manassas, VA) were plated at 2×10^5 cells/dish onto 35 mm glass-bottom microscope dishes (Matek, Ashland, MA) and allowed to incubate overnight (5% CO_2, 37 °C). The culture medium was then removed, and the cells were washed three times with phosphate buffered saline (PBS). The cell fixation and permeabilization were carried out as described by Pathak et al.[15] A 1.5 mL aliquot of a solution of 4% paraformaldehyde in PBS was added to cells for 10 min at room temperature, followed by rinsing three times with PBS, incubation with a 0.2% Triton solution in PBS for 10 min, and washing with PBS. After fixation, the cells were stored in PBS at 4 °C until use.

Single Particle Imaging and Tracking. Single particle imaging and tracking were performed on a customized wide-field epifluorescence microscope described as follows. The 488 nm laser beam from an argon laser is guided onto the epi-illumination port of an inverted fluorescence microscope (Olympus IX-71). Inside the microscope, the laser beam is reflected by a 500 nm long-pass dichroic mirror (Chroma 500 DCLP) and focused onto the rear aperture of a high numerical aperture objective (Olympus Ach, 100×, 1.25 NA, Oil). The laser excitation at the sample focal plane exhibits a fairly Gaussian profile with a full width at half-maximum of ∼5 μm. Typical laser intensities employed were ∼500 W/cm^2 in the center of the laser spot in the sample plane, as estimated based on the measured laser power, size of the excitation spot, and transmission of the objective. Nanoparticle fluorescence is collected by the objective lens, filtered by the combination of two 500 nm long-pass filters, and then refocused by an achromat lens onto a back-illuminated frame transfer CCD camera (Princeton Instruments, PhotonMAX: 512B), yielding a pixel resolution of 105 nm/pixel. An *xyz* piezoelectric scanning stage (P-517.3CL, Polytec PI) was used to center particles within the laser focal spot and for fine adjustment of focus. Acquisition rates of 33 or 50 images per second were employed. An overall microscope fluorescence detection efficiency of 3−5% was determined using nile red loaded polystyrene spheres (Invitrogen) as standards. Single nanoparticle fluorescence cross sections were determined by comparison of single nanoparticle fluorescence intensity to that of nile red loaded latex beads (Invitrogen). Determination of the lateral (*x*,*y*) position, width, and integrated intensity of the fluorescence spots was performed using custom scripts written for Matlab (Mathworks, Natick, MA). For the single particle tracking of PFBT nanoparticles undergoing Brownian motion in glycerol, a drop (∼50 μL) of nanoparticles suspended in glycerol at a concentration of 15 pM was placed between two cleaned microscope coverslips. For tracking of individual PFBT nanoparticles in a cell, 0.5 mL of a 4:1 glycerol/PBS solution, containing bovine serum albumin (BSA) (1 mg/mL) and PFBT nanoparticles (20 pM), was added into the prepared microscope dishes containing fixed cells and allowed to incubate for 12 h prior to imaging.

Results and Discussion

An aqueous suspension of nanoparticles roughly 15 nm in diameter was prepared from the conjugated polymer PFBT. AFM images, polymer chemical structure, UV−vis absorption and fluorescence spectra, and fluorescence microscopy of single particles are shown in Figure 1. PFBT was selected due to its excellent photostability and high absorption cross section at the 488 nm excitation wavelength employed in the tracking experiments.[12] An estimated optical absorption cross section (per 15 nm diameter particle) of 2.8×10^{-13} cm^2 at 488 nm was

(15) Pathak, S.; Cao, E.; Davidson, M. C.; Jin, S. H.; Silva, G. A. *J. Neurosci.* **2006**, *26*, 1893–1895.

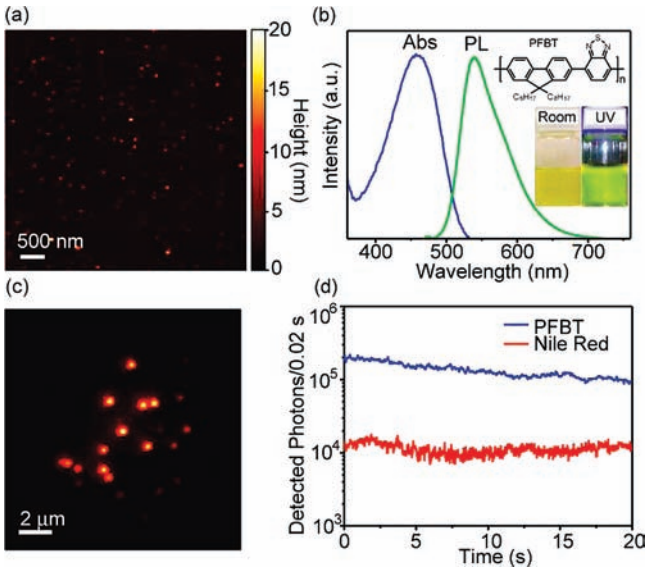

Figure 1. (a) AFM image of PFBT nanoparticles. (b) The absorption and fluorescence ($\lambda_{ex} = 475$ nm) spectra PFBT nanoparticles suspended in water, chemical structure of fluorescent conjugated polymer PFBT, and the photograph of PFBT nanoparticles suspended in water under room light and UV light illumination. (c) A fluorescence image of single PFBT nanoparticles immobilized on a glass coverslip. (d) Photobleaching trajectory (photons detected per 20 ms exposure versus time) of a single PFBT nanoparticle (blue line) and 20 nm nile red loaded polystyrene bead (red line).

determined.[12] The fluorescence quantum yield of the nanoparticles was determined to be 7%, corresponding to a fluorescence cross section of roughly 2.0×10^{-14} cm^2, which is at least 2 orders of magnitude higher than that of typical dyes and at least an order of magnitude higher than that of other <20 nm diameter fluorescent particles.[12]

To experimentally evaluate the particle brightness and the photostability at the single particle level under conditions employed for single particle tracking, particles were dispersed on a glass coverslip and imaged with a CCD-equipped inverted fluorescence microscope at an acquisition rate of 50 Hz. Bright, near-diffraction-limited fluorescence patterns were observed, and the detected photons per particle per image typically ranged between 1×10^6 and 1×10^5 for several hundred consecutive images (Figure 1c, d). Analysis of 20 typical single particle fluorescence intensity trajectories yielded an average of $\sim 10^9$ total photons emitted per particle (roughly 5×10^7 photons detected), with some particles emitting more than 10^{10} photons, and a per particle emission rate of ~1 GHz (corresponding to nearly saturated emission), in agreement with prior results.[12] These figures of merit are encouraging for improving the spatiotemporal resolution of fluorescence-based particle tracking, since, at high acquisition rates, the tracking uncertainty is largely determined by the saturated emission rate.

An initial estimate of the tracking uncertainty based on per-particle fluorescence intensity levels was obtained as follows. Assuming the tracking uncertainty is due to a combination of photon counting noise and the focal characteristics of the imaging setup, the tracking uncertainty δ is given by the expression,[16]

$$\delta = \sqrt{\frac{\sigma^2}{N} + \frac{a^2/12}{N} + \frac{8\pi\sigma^4 b^2}{a^2 N^2}} \qquad (1)$$

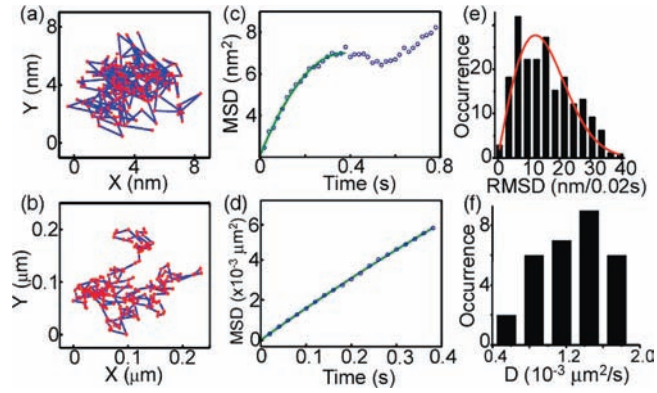

Figure 2. (a) 2-D trajectory of one stationary single PFBT nanoparticle adhered to a coverslip. (b) 2-D trajectory of a single particle diffusing in glycerol. (c) MSD versus time curve for the stationary particle. (d) MSD versus time curve for the particles diffusing in glycerol. The green lines represent a quadratic fit. The diffusion coefficient is 0.0013 μm^2/s. (e) Histogram of per-frame displacements and fit to 2D Gaussian. (f) Histogram of diffusion coefficients.

where σ is the width of the point spread function, a is the pixel size, b is the background noise, and N is the number of detected photons per image. Based on the measured 315 nm width (fwhm) of the single particle fluorescence spot, typical number of detected photons per image $N = 2 \times 10^5$, $a = 105$ nm, and $b = 17$, an estimated tracking uncertainty of better than 0.3 nm is obtained. The second and third terms in the above expression contribute less than 10% of the estimated tracking uncertainty, indicating that the expected contribution of pixel size and background noise to the tracking uncertainty is minimal.

Particle tracking resolution was experimentally determined by performing 2D tracking measurements of stationary particles deposited on a glass coverslip. A representative 2D trajectory and analysis are shown in Figure 2. Several hundred sequential fluorescence microscopy images were acquired at an acquisition rate of 50 images per second, and the particle position was determined by nonlinear least-squares fitting of the fluorescence spot associated with each particle in the image.[17,18] As an alternative to the common procedure of fitting to a 2D Gaussian function or Airy pattern to the fluorescence spot, a faster two-step fitting procedure was employed, in which the intensity data were alternately summed along the x and y axes, and 1D Gaussian functions were fit to the summed data. Initial analysis of a 200 point trajectory yielded an estimated tracking uncertainty of 4.6 nm, as given by the root-mean-square displacement per frame, rms $= \langle (x_{i+1} - x_i)^2 + (y_{i+1} - y_i)^2 \rangle^{1/2}$. However, comparison of the trajectories of two separate particles in the same set of images indicated highly correlated motion, likely due to the vibration of the imaging apparatus. After correcting the trajectory for the vibration by subtracting the position fluctuations of one particle from the other particle, a root-mean-square displacement per frame of 1.9 nm was obtained. Since the per-frame rms displacement of the vibration-corrected trajectory includes contributions from photon counting noise from two particles, the estimated tracking uncertainty per particle is 1.3 nm. Interestingly, the mean square displacement, $MSD(\tau) = \langle |r(t + \tau) - r(t)|^2 \rangle$, of the 2D vibration-corrected trajectories of the stationary particles is not flat (as would be expected for stationary particles) but rather increases linearly for ~400 ms

(16) Thompson, R. E.; Larson, D. R.; Webb, W. W. *Biophys. J.* **2002**, *82*, 2775–2783.
(17) Cheezum, M. K.; Walker, W. F.; Guilford, W. H. *Biophys. J.* **2001**, *81*, 2378–2388.
(18) Yildiz, A.; Selvin, P. R. *Acc. Chem. Res.* **2005**, *38*, 574–582.

and then plateaus (Figure 2c). This result was confirmed repeatedly and could be indicative of internal dynamics of the nanoparticle, such as intermittent quenching of the fluorescence in regions of the nanoparticle by reversibly photogenerated defects in the conjugated polymer, as has been observed in the fluorescence intensity trajectories of single conjugated polymer chains.[19] The ~1 nm tracking resolution determined at a temporal resolution of 20 ms is consistent with the estimated resolution based on signal level. Based on literature values, the saturated emission rate of the PFBT nanoparticles is roughly 2−3 orders of magnitude higher than that of colloidal semiconductor quantum dots,[3] which should result in a factor of roughly 10−30 improvement in tracking accuracy. A side-by-side comparison of the brightness of ~15 nm diameter PFBT nanoparticles and 20 nm nile red loaded polystyrene nanoparticles was performed (Figure 1d), indicating that the PFBT nanoparticles brightness is ~10 times higher than that of the dye-loaded nanoparticle. Since each polystyrene bead contained ~200 dye molecules, the brightness of the PFBT dots is roughly equivalent to 2000 dye molecules under these imaging conditions.

2D particle tracking was demonstrated on CPNs undergoing Brownian motion in a glycerol/water solution. A small amount of glycerol/water solution (>98% glycerol) containing ~15 nm diameter PFBT particles was sandwiched between two microscope coverslips and imaged at a rate of 50 Hz as described above. An *xyz* piezoelectric scanning stage was translated in the *xy* plane until a particle was located and roughly centered in the laser beam, followed by adjustment of the *z* position to bring the particle approximately into focus, at which time the CCD was set to acquire 1000 sequential images at a rate of 50 Hz. Typically, >300 images were acquired before the particle drifted too far above or below the focal plane to permit accurate determination of particle position. For the cases in which the particle remained in the focal plane for 1000 images (20 s), the photons detected per nanoparticle per image typically remained above 100 000 for the entire experiment, as required for high resolution, long-term tracking. The particle trajectories (Figure 2b) were obtained from the images by fitting to Gaussian functions as described above. Fitting a 2D Gaussian to the per-frame displacement histogram (Figure 2e) yielded $\sigma = 12$ nm, which is primarily due to diffusion. To determine the diffusion constant, MSD as a function of lag time (Figure 2d) was fit to the equation

$$\mathrm{MSD}(\tau) = 4\pi D\tau + (v\tau)^2 \qquad (2)$$

where D is the diffusion constant and v is the drift velocity. The results were analyzed for several particles, yielding a negligible drift velocity and diffusion constants ranging from 4×10^{-4} to 2×10^{-3} μm^2/s (Figure 2f), which is somewhat smaller than the theoretical diffusion constant obtained from the Stokes−Einstein relation. The discrepancy may be due to some particle swelling by the glycerol as well as the additional hydrodynamic drag known to occur for charged colloids at low ionic strength.[20] The MSD curve can be extrapolated to zero lag time to estimate the tracking uncertainty, yielding a value ranging between 1 and 4 nm. This estimate of the tracking uncertainty is consistent with the 1−2 nm tracking uncertainty obtained based on the rms displacement per frame for stationary particles.

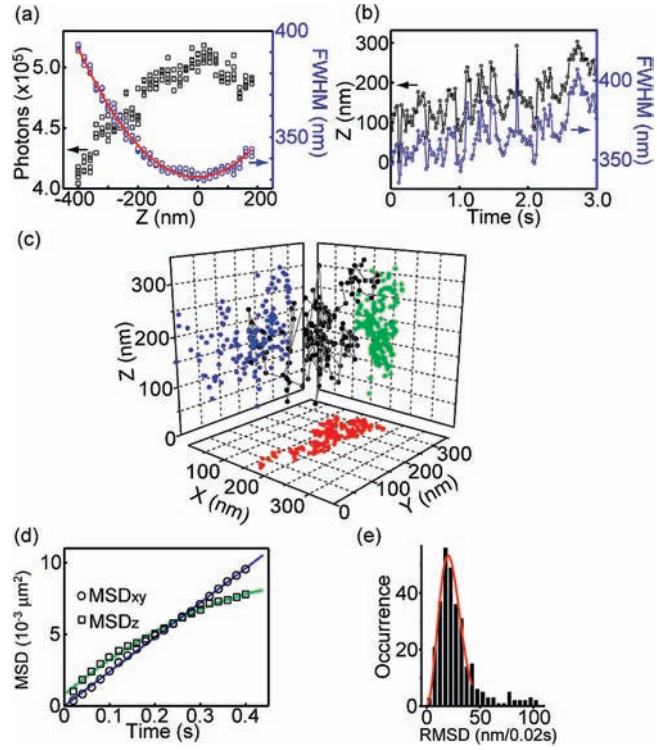

Figure 3. The intensity (black squares) and width (blue circles) versus *z* axis position curves were obtained by displacing PFBT nanoparticles in 20 nm steps (a), with the quadratic fit (red line). (b) The width and the *z* axis position versus time curves of one PFBT nanoparticle diffusing in glycerol solution. (c) The 3D trajectory and its projection onto the *xy*, *yz*, and *xz* planes. (d) MSD for the above tracked PFBT nanoparticle at different time intervals. The squares show the MSD along the axial (*z*) direction, and the circles show the lateral (*x,y*) MSD. The green and blue lines correspond to the quadratic fits of the axial and lateral MSD, yielding diffusion coefficients of 0.0038 and 0.0019 μm^2/s, respectively. (e) Histogram of per-frame displacements for the 3D trajectory and 3D Gaussian fit.

Tracking of particles in 3D was performed, employing a variant of defocused imaging to determine the axial (*z*) position of the nanoparticle.[4,21] Trajectories and analysis are shown in Figure 3. The objective focal plane was displaced several hundred nanometers from the particle of interest, and particles were imaged as described above. The lateral positions and widths of the fluorescence spots were determined by Gaussian fitting, as described above. The width of the fluorescence spot was analyzed to determine the axial position as follows. To experimentally determine the relationship between the width of the defocused point spread function and nanoparticle axial position, the PFBT nanoparticles were immobilized on a coverslip and the axial position was systematically varied using an *xyz* piezoelectric stage, which was driven with a staircase waveform generated by a programmable function generator. The sample was then displaced in 20 nm steps, and the resulting spot widths were analyzed using the particle tracking routine (Figure 3a). The fluorescence spot width W as a function of axial position z, in units of nanometers, was fit to a parabola,

$$W = az^2 + bz + c \qquad (3)$$

yielding a good fit for the parameters $a = 3.9 \times 10^{-4}$, $b = 2.5 \times 10^{-3}$, $c = 330$. Using this equation, the axial position was

(19) VandenBout, D. A.; Yip, W. T.; Hu, D. H.; Fu, D. K.; Swager, T. M.; Barbara, P. F. *Science* **1997**, *277*, 1074–1077.

(20) (a) Dai, S.; Tam, K. C.; Jenkins, R. D. *Macromol. Chem. Phys.* **2001**, *202*, 335–342. (b) vanRoij, R.; Hansen, J. P. *Phys. Rev. Lett.* **1997**, *79*, 3082–3085. (c) Sasaki, S. *Colloid Polym. Sci.* **1984**, *262*, 406–408.

(21) Speidel, M.; Jonas, A.; Florin, E. L. *Opt. Lett.* **2003**, *28*, 69–71.

determined from the width of the fluorescence spot. Based on the standard deviation of 2.4 nm in the ~350 nm average width obtained for a fit for a spot roughly 240 nm from the focal plane, error propagation analysis applied to the above equation yields an uncertainty in axial position of 25 nm. The estimation of the axial position of a defocused particle from the fluorescence spot width was combined with lateral position measurements to determine the 3D trajectory of a particle undergoing Brownian motion (Figure 3c). The axial and the lateral MSD exhibited a linear dependence on lag time, as expected for Brownian motion. The axial diffusion coefficient, D_z, and the lateral diffusion coefficient, D_{xy}, were obtained from their respective MSD curves, resulting in 3.8×10^{-3} and 1.9×10^{-3} $\mu m^2/s$, respectively (Figure 3d). Extrapolation of the axial MSD to the zero lag time shows an estimated tracking uncertainty of 19 nm, consistent with the result obtained by error propagation. Figure 3e shows the histogram of per-frame displacements, which is fit to a Gaussian function, giving $\sigma = 14.3 \pm 0.3$ nm, which is largely attributable to axial tracking uncertainty. These results indicate that, for 3D tracking of the ~15 nm diameter PFBT nanoparticles, a lateral (x,y) resolution of <5 nm and an axial (z) resolution of ~20 nm can be achieved at an acquisition rate of 50 Hz using a conventional fluorescence video microscopy apparatus. It is expected that further improvements in temporal and axial resolution could be obtained using more advanced tracking methods.[22]

Tracking of PFBT nanoparticles was performed in the vicinity of fixed and permeabilized mouse macrophage-like J774 cells, at an acquisition rate of 33 Hz, in 4:1 glycerol/phosphate buffered saline (PBS) solution. In the absence of bovine serum albumin (BSA), the nanoparticles accumulated on the surface of the cell membrane within a few minutes. Addition of 1% BSA was found to greatly reduce nonspecific binding to the membrane, likely due to adhesion of the protein to the nanoparticle surface. Figure 4 shows a brightfield transmission image of the cell, together with nanoparticle trajectories and analysis. When the edge of the cell was placed near the center of the imaging area, particles were visible in the interior of the cell, adhered to the membrane, and outside the cell, and a sequence of images was acquired. As compared to the results obtained in nearly pure glycerol, the reduced viscosity of the 80% glycerol resulted in higher per-frame displacements of the particles. The motion of the particles during each acquisition interval resulted in variable spot shapes that reduced the accuracy of Gaussian fitting, so a centroid algorithm was used to track the particles.[17] In the trajectories and MSD curves (Figure 4b−d), several distinct phenomena are observed. The particle inside the cell (Figure 4a, b) switches between free Brownian motion, with a corresponding linear increase in the MSD curve, and confined or bound behavior resulting in a relatively flat MSD. Additional, longer trajectories would be needed to differentiate between confined diffusion behavior and binding−unbinding behavior. Another particle apparently adhered to the cell membrane and exhibited low amplitude (15 nm) oscillatory motion, while the particle outside the cell exhibited free Brownian motion.

Conclusion

In conclusion, we have demonstrated that small (~15 nm diam) PFBT nanoparticles exhibit intense fluorescence that permits 3D tracking with nanometer lateral spatial resolution and video rate temporal resolution. The saturated per particle emission rate is typically 10^9 photons/s, roughly 2−3 orders of magnitude higher than that of other luminescent nanoparticles of similar size, resulting in a factor of 10−30 improvement in spatial resolution for emission rate-limited tracking experiments. The high fluorescence cross section of the particles is useful for tracking in complex environments exhibiting high autofluorescence and scattering that often drowns out the signal of dyes and other small nanoparticle labels. Free Brownian motion of the nanoparticles in glycerol was observed with nanoscale resolution at a 50 Hz acquisition rate, and complex motion in cells was observed. Based on these results, we conclude that the extraordinary brightness of CPNs under one-photon and two-photon excitation[15] should be useful for a broad range of particle tracking applications requiring small particles, video rate or higher temporal resolution, and nanometer spatial resolution. It is likely that additional efforts to improve particle brightness and photostability by employing improved polymers or by encapsulation could yield further improvements in tracking resolution.

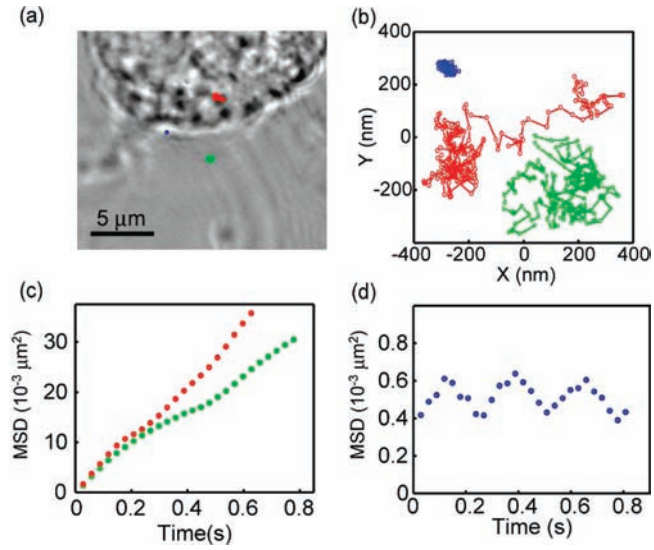

Figure 4. (a) Bright field transmission image of a fixed cell. The color marks indicate the locations of the particles. Blue corresponds to a particle bound to the membrane, green corresponds to a particle outside the cell, and red corresponds to the cell interior. (b) The trajectories for the three particles. (c) MSD curves of the above tracked PFBT nanoparticle inside cell (red circles) and outside cell (green circles), corresponding to diffusion constants of 3.3×10^{-3} and 3.6×10^{-3} $\mu m^2/s$, respectively. (d) MSD curve of particle adhered to the membrane.

Acknowledgment. The authors gratefully acknowledge financial support from the NSF/EPSCoR under Grants No. 2001RII-EPS-0132573 and 2004RII-EPS-0447660, NSF (CAREER) CHE-0547846, and NIH Grant No. 1R01GM081040. We also thank Thompson Mefford and Steven Saville for performing zeta potential measurements.

Supporting Information Available: Additional figures providing experimental details and a particle tracking video. This material is available free of charge via the Internet at http://pubs.acs.org.

JA907228Q

(22) Cang, H.; Xu, C. S.; Yang, H. *Chem. Phys. Lett.* **2008**, *457*, 285–291.